

Hepta-coordinate halocarbonyl molybdenum(II) and tungsten(II) complexes as heterogeneous polymerization catalysts

Jorge Gimenez^a, Carla D. Nunes^a, Pedro D. Vaz^a, Anabela A. Valente^b,
Paula Ferreira^c, Maria José Calhorda^{a,*}

^a Department of Chemistry and Biochemistry, CQB, Faculty of Science, University of Lisbon, C8 Campo Grande, 1749-016 Lisboa, Portugal

^b Department of Chemistry, CICECO, University of Aveiro, Campus de Santiago, 3810-193 Aveiro, Portugal

^c Department of Ceramics and Glass Engineering, CICECO, University of Aveiro, Campus de Santiago, 3810-193 Aveiro, Portugal

Received 27 February 2006; received in revised form 6 April 2006; accepted 8 April 2006

Available online 5 June 2006

Abstract

[MX₂(CO)₃(DAB)] (M=Mo, W; X=I, Br) (**5–8**) complexes bearing the 1,4-diazobutadiene (DAB) ligand RN=C(Ph)–C(Ph)=NR [R=(CH₂)₃Si(OEt)₃] were immobilized in MCM-41 mesoporous silica. The tethering, stepwise procedure started with treatment of the MCM-41 mesoporous material with a toluene solution of the 1,4-diazobutadiene ligand, under reflux. The molybdenum and tungsten organometallic cores were subsequently introduced into the ligand-silicas by pore volume impregnation of a solution of the complexes [MX₂(CO)₃(NCMe)₂] (M=Mo, W; X=Br, I). The modified materials were extensively characterized by several techniques, such as FTIR, solid-state MAS and CP MAS NMR (¹³C, ²⁹Si), powder XRD, and nitrogen adsorption–desorption measurements. These new materials (containing 2.6–2.9 wt.% Mo or 0.4–0.6 wt.% W) catalyze the ring-opening metathesis polymerization (ROMP) of norbornene (NBE) and norbornadiene at 328 K, in contrast with the very low activity exhibited by the precursor complexes and with their behavior at lower temperature. Addition of AlCl₃ as a co-catalyst enhanced the catalytic performance of the material MCM-DAB-MoBr₂ (**12**) in the ROMP of NBE.

© 2006 Elsevier B.V. All rights reserved.

Keywords: Molybdenum; Tungsten; MCM-41; Polymerization; DAB ligands; Hepta-coordination; Catalysis

1. Introduction

Organometallic complexes can efficiently and selectively catalyze many reactions and are widely applied in industrial processes. One drawback of such homogeneous catalysts is the difficulty of separating the products from the reaction solution and recovering and recycling the catalyst. Therefore, the possibility of incorporating complexes in materials to yield heterogeneous catalysts has opened new possibilities in recent years [1,2]. Seven-coordinate Mo(II) complexes [MX₂(CO)₃L₂] (M=Mo, W; X=halogen) and their derivatives, obtained by replacing the labile nitrile ligands, have been extensively investigated [3–5]. Their synthesis [6–9], structures [10,11] and properties have been studied since they were reported for the first time by Nigam and Nyholm in 1957 [12], and they have been shown to exhibit catalytic activity [13,14]. Complexes

[M(CO)₃X₂(NCMe)₂] have been successfully used by Baker and co-workers in the ring-opening metathesis polymerization (ROMP) of norbornene (NBE) and norbornadiene (NBD) [15,16] with satisfactory results, though some of the complexes were only active upon the addition of a Lewis acid, such as AlCl₃ or ZrCl₄. Szymańska-Buzar et al. carried out the study of ROMP reactions with seven-coordinate Mo(II) and W(II) complexes [17–19].

The micelle templated silicas MCM-41 (hereafter denoted as MCM) belong to the M41S family developed by Mobil Corporation in 1992 [20,21], and display a set of properties, such as a stable and ordered mesoporous structure, large surface area (usually >1000 m² g⁻¹), and narrow pore size distribution, which make them ideal for hosting molecules of various sizes, shapes and functionalities. These features are suitable for the inclusion of organometallic complexes and have led to significant developments, among others, in the fields of catalysis, adsorption/sorption, separation, sensors, optically active materials [1,22]. The number of papers describing this type of chemistry has been growing each year [1,2,23].

* Corresponding author. Tel.: +351 217500196; fax: +351 217500088.
E-mail address: mjc@fc.ul.pt (M.J. Calhorda).

In the present work, bis(acetonitrile) Mo(II) and W(II) complexes were used as precursors for the immobilization of organometallic species in MCM, by a tethering approach. In the first step, the triethoxysilyl-*N*-substituted 1,4-diazobutadiene (DAB) ligand was grafted on the host material MCM-41, and was subsequently allowed to react with the organometallic complexes $[MX_2(CO)_3(NCMe)_2]$ ($M = Mo, W; X = Br, I$). The derivatized materials were fully characterized and tested as catalysts for the ring-opening metathesis polymerization (ROMP) of norbornadiene (NBD) and norbornene (NBE).

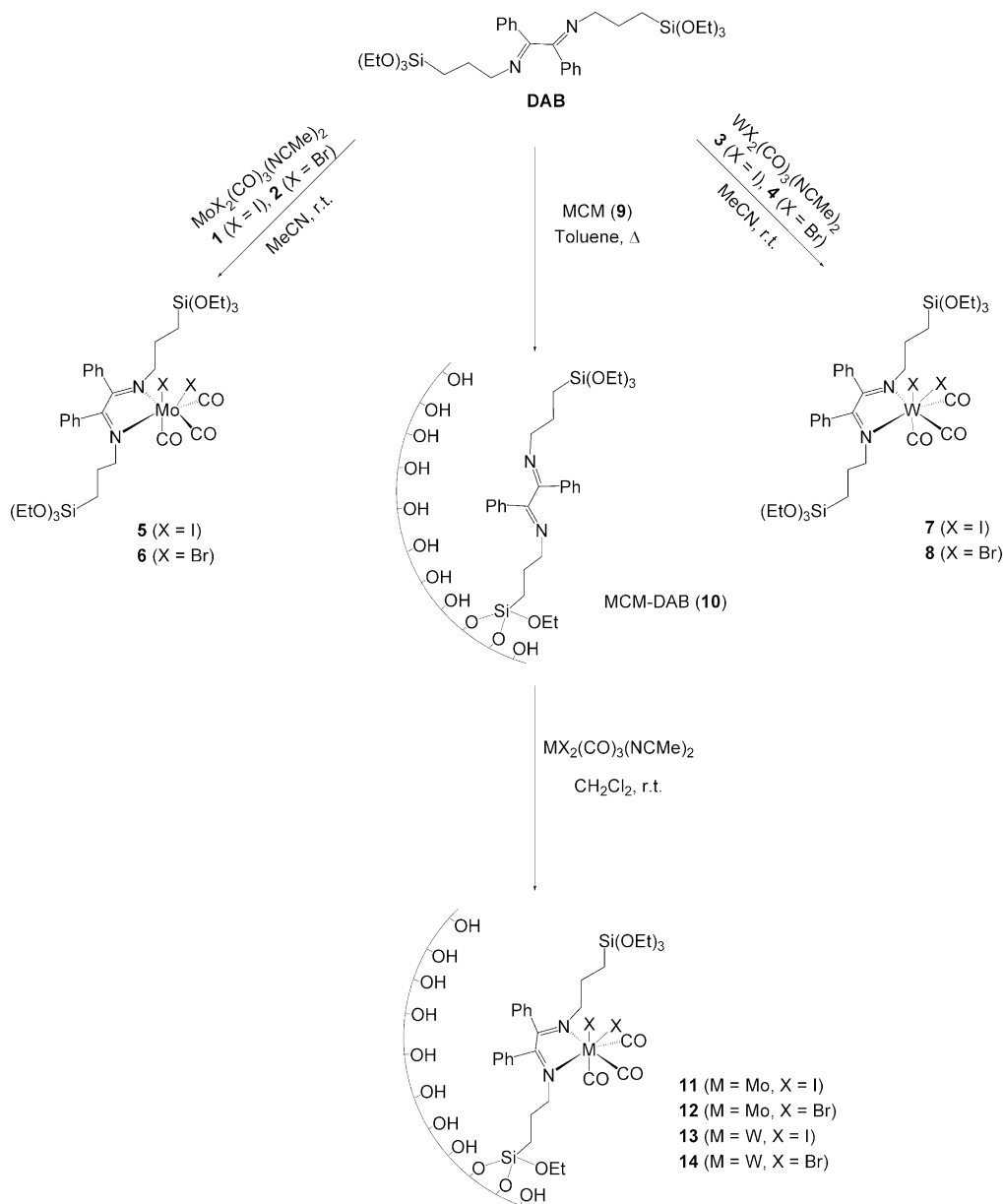
2. Results and discussion

2.1. The organometallic complexes

The functionalized triethoxysilyl ligand $RN=C(Ph)-C(Ph)=NR$ (DAB) [$R=(CH_2)_3Si(OEt)_3$] was prepared by the reaction

of benzil $[C_6H_5(CO)(CO)C_6H_5]$ with two equivalents of (3-aminopropyl)triethoxysilane, according to a well-known procedure [24]. The precursor complexes $[MX_2(CO)_3(NCMe)_2]$ ($M = Mo, W; X = I$ or Br) (1–4) [25] were allowed to react with one equivalent of the DAB ligand, affording the complexes $[MX_2(CO)_3\{Ph-DAB-CH_2Si(OEt)_3\}_2]$ ($M = Mo, W; X = I$ or Br) (5–8) by displacement of both labile acetonitrile ligands and in good yield. These complexes were subsequently immobilized on the MCM-41 host material, as outlined in Scheme 1 [24,26].

Both the ligand DAB [24] and the precursor complexes 1–4 [25] have been characterized elsewhere and therefore will not be discussed here. The 1H NMR spectrum of $[MoI_2(CO)_3\{Ph-DAB-CH_2Si(OEt)_3\}_2]$ (5) shows a multiplet in the range $7.36 < \delta < 7.95$ ppm assigned to the phenyl groups, as well as multiplet signals at $\delta = 3.47$ – 3.52 ppm (NCH_2), 1.93 – 1.98 ppm ($CH_2CH_2CH_2$) and a broad singlet at 0.71 ppm ($SiCH_2$) for the propyl chains. The presence of ethoxy groups



Scheme 1.

Table 1
FTIR wavenumbers of $\nu_{\text{C=O}}$, $\nu_{\text{C}\equiv\text{N}}$ and $\nu_{\text{C=N}}$ modes for complexes **1**, **2**, **5**, and **6**

Complex	$\nu_{\text{C=O}}$ (cm^{-1})	$\nu_{\text{C}\equiv\text{N}}$ (cm^{-1})	$\nu_{\text{C=N}}$ (cm^{-1})
[MoI ₂ (CO) ₃ (NCMe) ₂] (1)	1921 (vs), 2016 (vs), 2072 (m)	2276 (vs), 2304 (vs)	–
[MoI ₂ (CO) ₃ (DAB)] (5)	1946 (m), 2017 (m), 2067 (vw)	–	1637 (s)
[MoBr ₂ (CO) ₃ (NCMe) ₂] (2)	1943 (vs), 2021 (vs), 2091 (vw)	2279 (s), 2309 (m)	–
[MoBr ₂ (CO) ₃ (DAB)] (6)	1930 (vs), 2011 (s), 2063 (vw)	–	1635 (s)

is reflected by signals at $\delta=3.47$ – 3.52 ppm (OCH₂, convoluted with NCH₂) and 1.04 ppm (CH₃). These signals are slightly shifted relative to those of the free ligand DAB, which exhibits three multiplets at $\delta=7.32$ – 7.50 ppm, 7.57– 7.75 ppm, and 7.88– 7.93 ppm (aromatic protons), and resonances at $\delta=3.40$ – 3.44 ppm, 1.76– 1.86 ppm and 0.60– 0.68 ppm assigned to the NCH₂, CH₂CH₂CH₂, and SiCH₂, respectively; the ethoxy groups peaks are observed at $\delta=3.73$ – 3.84 ppm (OCH₂CH₃) and 1.15– 1.24 ppm (OCH₂CH₃) [24].

The absence of resonances from the acetonitrile ligands indicates the coordination of the ligand to the molybdenum centre. This is confirmed by the ¹³C NMR spectrum, displaying one resonance at $\delta=166.7$ ppm, due to the N=C atoms, and signals at $\delta=128.9$ ppm, 128.0 ppm and 127.2 ppm, assigned to the aromatic carbon atoms. Signals from the propyl chains appear at $\delta=68.7$ ppm (NCH₂), 21.7 ppm (CH₂CH₂CH₂) and 13.1 ppm (SiCH₂). The ethoxy groups have resonances at $\delta=58.1$ ppm (OCH₂) and 20.4 ppm (CH₃).

The FTIR spectrum of [MoI₂(CO)₃{Ph-DAB-CH₂Si(OEt)₃}₂] (**5**) shows the displacement of the labile acetonitrile ligands during the synthesis, as evidenced by the absence of the $\nu_{\text{C}\equiv\text{N}}$ stretching modes at ca. 2300 cm^{-1} (Table 1). A new band at 1637 cm^{-1} is clearly observed arising from the new $\nu_{\text{C=N}}$ mode, and two broad and intense bands assigned to $\nu_{\text{Si-O}}$ stretching modes appear at 1116 cm^{-1} and 1024 cm^{-1} . In the free ligand DAB, the band corresponding to the $\nu_{\text{C=N}}$ mode is observed at 1647 cm^{-1} . The shift of the $\nu_{\text{C=N}}$ band to lower frequency is indicative of the coordination of DAB to the complex [MoI₂(CO)₃(MeCN)₂] (**1**), with weakening of the C=N bond. For complex **6** [MoBr₂(CO)₃{Ph-DAB-CH₂Si(OEt)₃}₂], comparable changes in the vibrational spectrum occur, but the

$\nu_{\text{C=N}}$ mode is shifted to lower wavenumbers than in **5**. This suggests a stronger M–N bond of the metal centre to DAB in the dibromo complex **6** than in the diiodo one **5**. The bands assigned to the $\nu_{\text{Si-O}}$ stretching modes in complex **6** are observed at 1167 cm^{-1} and 1075 cm^{-1} . Some small changes are also observed for the $\nu_{\text{C=O}}$ bands upon chelation of the DAB ligand to the bis(acetonitrile) Mo(II) complexes **1** and **2** and for the corresponding W(II) complexes, as shown in Table 1. This indicates that the formation of Mo–N bonds affects to some extent the strength of the Mo–C bonds by changing the amount of π -backdonation to the carbonyl ligands.

The spectroscopic characterization of all the complexes **5–8** by ¹H, ¹³C NMR and FTIR led to similar results (see Section 4 for remaining complexes).

2.2. The functionalized materials

Two lots of samples of MCM-41 host material **9** or **9*** (* denotes a different lot) were prepared by a template approach as described previously [24]. This material was then derivatized by grafting of the phenyl-substituted 1,4-diazobutadiene ligand DAB onto the silica-matrix mesoporous host material, in toluene, overnight. After filtration, the solids were washed thoroughly with dichloromethane, and dried in vacuum at 100 °C for several hours, originating materials **10** or **10***, respectively. This procedure has been reported by I.S. Gonçalves and co-workers to immobilize dioxomolybdenum(VI) species using the ligand-silica system **10**, which originated active catalysts for the epoxidation of olefins [24,26]. In this work, **10** or **10*** were allowed to react with an excess of the bis(acetonitrile) complexes (**1–4**) in methylene chloride, overnight, at room temperature, and

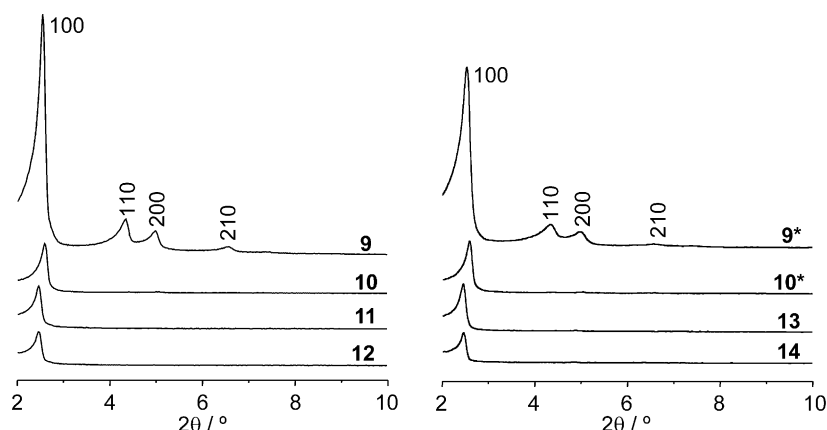


Fig. 1. Powder XRD patterns for materials MCM (**9** and **9***), MCM-DAB (**10** and **10***), MCM-DAB-MoI₂ (**11**), MCM-DAB-MoBr₂ (**12**), MCM-DAB-WI₂ (**13**) and MCM-DAB-WBr₂ (**14**).

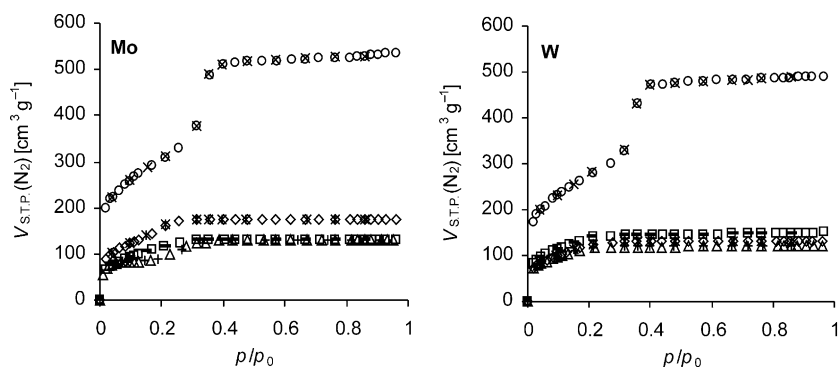


Fig. 2. Nitrogen adsorption (○) (**9** and **9***); (◇) (**10** and **10***); (□) (**11** and **13**); (Δ) (**12** and **14**) and desorption (×) (**9** and **9***); (*) (**10** and **10***); (–) (**11** and **13**); (+) (**12** and **14**) isotherms at 77 K.

after filtering and drying, afforded the composite materials **11**, **12** and **13**, **14**, respectively. In the case of **11** and **12**, the molybdenum loadings were 2.6 wt.% and 2.9 wt.% (0.27 mmol g^{-1} and 0.30 mmol g^{-1}), respectively. For the tungsten containing materials **13** and **14**, the results show metal loadings of only 0.4 wt.% and 0.6 wt.% (0.05 mmol g^{-1} and 0.09 mmol g^{-1}), respectively. These results indicate that the immobilization of the tungsten complexes was not very successful, although several attempts were pursued.

The new materials were characterized by powder XRD diffraction, adsorption studies, FTIR and solid-state ^{13}C and ^{29}Si NMR.

The powder XRD patterns for the process-control are shown in Fig. 1. The powder pattern of the MCM parent, calcined material **9**, clearly shows four reflections in the 2θ range $2\text{--}10^\circ$, indexed to a hexagonal cell as (1 0 0), (1 1 0), (2 0 0) and (2 1 0). The d -value of the (1 0 0) reflection was 34.6 \AA (34.8 \AA for material **9***), corresponding to a lattice constant of $a = 40.0 \text{ \AA}$ ($=2d_{100}/\sqrt{3}$) (40.2 \AA for material **9***). Upon functionalization of the walls of the parent host material **9** or **9*** with the diazobutadiene ligand DAB and subsequent inclusion of the metallic complexes (**1–4**), the powder patterns remain unchanged in what concerns the positions of the peaks assigned to the characteristic reflections, suggesting the retention of the long range hexagonal symmetry of the host material. However, a drastic reduction of the peaks intensities is clearly observed. This is not interpreted as a loss of crystallinity, but rather to a reduction in the X-ray scat-

tering contrast between the silica walls and pore-filling material, a situation well described in the literature [27,28].

Nitrogen adsorption studies at 77 K revealed that the pristine MCM samples (**9** and **9***) exhibit reversible type IV isotherms (Fig. 2), characteristic of mesoporous solids (pore width between 2 nm and 50 nm, according to the IUPAC) [29]. The calculated textural parameters (S_{BET} and V_t) of these materials agree with literature data (Table 2) [30,31]. The capillary condensation/evaporation steps of pristine MCM samples appear in the relative pressures range 0.26–0.4. The sharpness of this step reflects the uniform pore size.

The isotherms of the functionalized materials revealed much lower N_2 uptake, accounting for decreases in S_{BET} (52–63%) and V_t (67–76%). These results suggest that immobilization of the complexes on the internal silica surface was accomplished (Fig. 2, Table 2). This conclusion is also supported by the decrease of the p/p_0 coordinates of the inflection points of the isotherms upon post-synthesis treatments [32]. The height of the capillary condensation step, which is related to the volume of pore space confined by adsorbate film on the pore walls, is much smaller in the case of the modified MCM materials. Furthermore, the maximum of the PSD curve for MCM determined by the BJH method, d_{BJH} , decreases from 3.7 nm to less than 3 nm (Table 2).

The FTIR spectrum of the parent host material MCM **9** (Fig. 3) is similar to that of other mesoporous siliceous matrices [27,28]. The bands at 1235 cm^{-1} and 1087 cm^{-1} are assigned

Table 2
Textural parameters for host and composite materials from N_2 isotherms at 77 K

Sample	S_{BET} ($\text{m}^2 \text{ g}^{-1}$)	$\Delta S_{\text{BET}}^{\text{a}}$ (%)	V_{p} ($\text{cm}^3 \text{ g}^{-1}$)	$\Delta V_{\text{p}}^{\text{b}}$ (%)	$d_{\text{BJH}}^{\text{c}}$ (nm)
9	1106	–	0.83	–	3.7
10	526	52	0.27	67	2.9
11	411	63	0.20	76	2.9
12	467	58	0.23	72	2.9
9*	981	–	0.76	–	3.7
10*	438	55	0.20	74	2.7
13	494	50	0.23	70	2.5
14	420	57	0.19	75	2.6

^a Variation of surface area in relation to parent MCM.

^b Variation of total pore volume in relation to parent MCM.

^c Median pore width determined by the BJH method.

* MCM from a different lot.

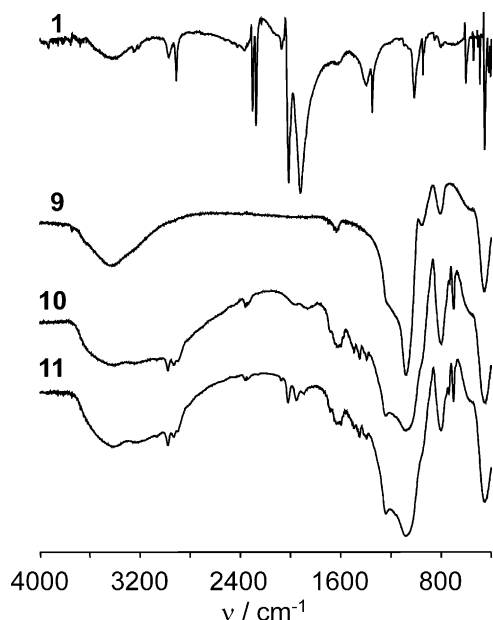


Fig. 3. FTIR spectra of $[\text{MoI}_2(\text{CO})_3(\text{NCMe})_2]$ (**1**), MCM (**9**), MCM-DAB (**10**) and MCM-DAB- MoI_2 (**11**).

to the ν_{asym} mode of the Si–O–Si framework, the corresponding ν_{sym} mode appearing at ca. 800 cm^{-1} . An absorption at 963 cm^{-1} is assigned to a $\delta_{\text{Si-O}}$ mode of the Si–OH groups [27,28]. The treatment of MCM **9** with DAB led to the derivatized material **10**, which presents new bands in the vibrational spectrum relative to that of **9**. The bands at 3067 cm^{-1} , 2978 cm^{-1} , 2927 cm^{-1} and 2891 cm^{-1} are assigned to $\nu_{\text{C-H}}$ modes of the ligand. The band at 1652 cm^{-1} can be assigned to the $\nu_{\text{C=N}}$ mode of the ligand (1647 cm^{-1} in free DAB), suggesting that the ligand was immobilized inside the pores of the host material without its structure being affected. The $\beta_{\text{C-H}}$ and $\nu_{\text{C=C}}$ modes of the ligand are responsible for a set of three bands at 1494 cm^{-1} , 1447 cm^{-1} and 1390 cm^{-1} . The presence of the carbonyl ligands in the immobilized complexes allows valuable information to be extracted from the vibrational spectra of the new materials, as the $\nu_{\text{C=O}}$ stretching mode is a very strong one. Chelation of the immobilized ligand **10** to the metal fragments $\text{MX}_2(\text{CO})_3$ ($\text{M}=\text{Mo}$; $\text{X}=\text{I}, \text{Br}$) is also deduced from the vibrational spectra. The appearance of the bands at 2073 cm^{-1} , 2022 cm^{-1} and 1954 cm^{-1} , assigned as the $\nu_{\text{C=O}}$ modes for **11**, denotes the presence of three coordinated carbonyl groups, and the retention of the organometallic $\text{M}(\text{CO})_3$ core during the immobilization procedure. The absence of the bands at 2276 cm^{-1} and 2304 cm^{-1} , corresponding to the $\nu_{\text{C}\equiv\text{N}}$ modes of the acetonitrile in the precursors, reflects their substitution by other ligands. Moreover, the $\nu_{\text{C=N}}$ mode of the DAB ligand is observed at 1631 cm^{-1} , a value lower than that of the free ligand, indicating chelation to the metal centre. In the case of **12**, the corresponding $\nu_{\text{C=O}}$ bands are observed at 2082 cm^{-1} , 2018 cm^{-1} and 1944 cm^{-1} , and the $\nu_{\text{C=N}}$ mode of the ligand at 1627 cm^{-1} .

The composite materials **13** and **14** containing W(II) (prepared from **10**^{*}) were found to exhibit similar spectroscopical features to those of the Mo(II) analogues (materials **11** and **12**),

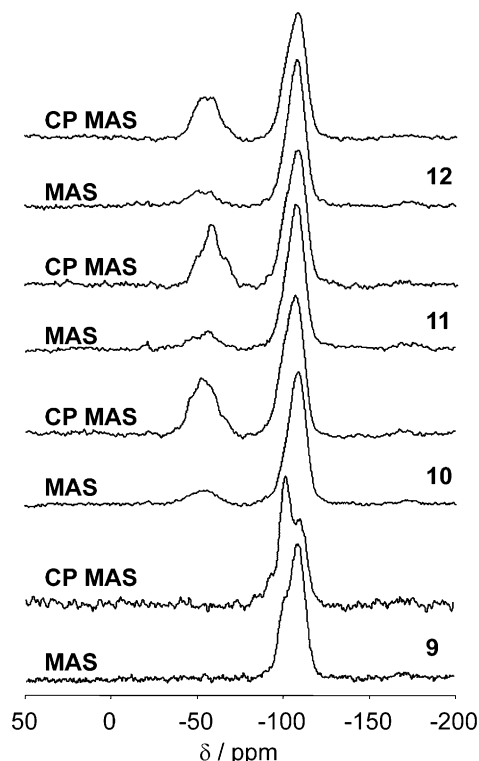


Fig. 4. ^{29}Si MAS and CP MAS NMR for materials MCM (**9**), MCM-DAB (**10**), MCM-DAB- MoI_2 (**11**) and MCM-DAB- MoBr_2 (**12**).

with absence of the $\nu_{\text{C}\equiv\text{N}}$ bands and the presence of bands assigned to the carbonyls, suggesting that the $\text{W}(\text{CO})_3$ fragments were also successfully immobilized inside the pores of the MCM host material.

All the materials were also characterized by ^{29}Si MAS and CP MAS NMR and ^{13}C CP MAS solid-state NMR spectroscopy. As shown in Fig. 4, the ^{29}Si MAS and CP MAS spectra present some changes reflecting the evolution of the tethering procedure during the preparation of the composite materials.

The spectra of material **9** show the presence of two convoluted resonances assigned to Q^3 and Q^4 ($Q^n = \text{Si}(\text{OSi})_n(\text{OH})_{4-n}$) at $\delta = -102.0\text{ ppm}$ and -109.0 ppm , respectively. Also a minimal amount of Q^2 species can be observed at $\delta = -92.5\text{ ppm}$. Upon grafting of the chelating ligand to the walls of the parent host material, the spectra of the new material **10** shows a reduction of the intensities of the resonances assigned to Q^2 and Q^3 species, owing to the silylation of the surface by nucleophilic substitution. Although the Q^3 sites are the most reactive, some remain unreacted at the surface, suggesting that they can be blocked to functionalization due to hydrogen bonding $(\text{SiO})_3\text{Si-OH} \dots \text{OH-Si}(\text{SiO})_3$ [29]. The spectra of materials **10**, **11** and **12** show three new convoluted signals in the -50 ppm to -58 ppm range. These resonances are associated with organosilica species T^1 , T^2 and T^3 , where $T^m = \text{RSi}(\text{OSi})_m(\text{OEt})_{3-m}$. The presence of these signals in the spectra is indicative of the successful introduction of the ligand DAB, and also shows that the ligand is covalently bound to the surface of the host material. The ^{29}Si NMR spectra of materials **11** and **12** are similar to that of **10**. In fact, since the ligand binds to the metal centres by

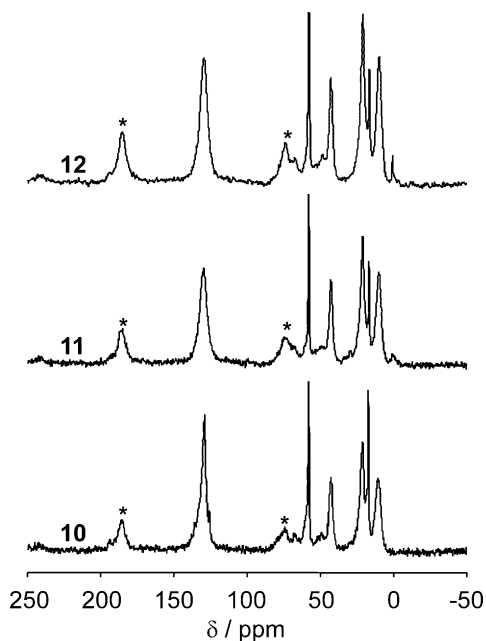


Fig. 5. ^{13}C CP MAS NMR for materials MCM-DAB (**10**), MCM-DAB-MoI₂ (**11**) and MCM-DAB-MoBr₂ (**12**).

the nitrogen atoms, no significant alterations of the silica atoms chemical shifts would be expected.

The ^{13}C CP MAS NMR of the functionalized material **10** is very similar to that of the free DAB ligand (liquid ^{13}C NMR), Fig. 5. Only a slight decrease in the intensity of resonances assigned to the SiO–CH₂CH₃ groups is observed, which is expected, since the binding of the ligand to the surface of the host material takes place by the hydrolysis of these groups.

The resonances due to the aromatic nuclei in materials **11** and **12** are also well described, despite the large width of the signal. Nevertheless, the solution ^{13}C NMR of complex **5** (and

6), described earlier in this work, made possible the observation of all signals. The resonances corresponding to the C=N and C≡O carbon atoms are not clear in the ^{13}C CP MAS NMR of materials **11** and **12**, owing to the overlapping of the spinside band and of the high relaxation time of the carbonyl groups. Despite this, the presence of such groups is confirmed by the corresponding FTIR spectrum (see above).

The solid-state NMR studies for the W(II) containing materials **13** and **14** led to the same conclusions found for composite materials **11** and **12**, as in the case of the FTIR results: a full description of spectral data can be found in Section 4.

2.3. Polymerization catalytic studies

The study of olefin polymerization catalyzed by Mo(II) and W(II) systems has received much attention over the last years [15–19]. Complexes **1–4** have already been tested for ROMP catalysis of NBE and NBD (polyNBE and polyNBD denote the corresponding polymer product). Metathesis polymerization of NBD is successfully carried out by complexes [MX₂(CO)₃(NCMe)₂] at room temperature for X = Br, whereas the diiodo requires a co-catalyst, such as ZrCl₄ or AlCl₃, in order to initiate polymerization [15 and references therein].

Complexes **5–8** did not catalyze the ROMP reactions of NBE and NBD at 298 K (see other conditions in Section 4). At 328 K, however, some catalytic activity was observed, yielding 1–8% polymer (Table 3). Complex **6** (M = Mo, X = Br) presents a slightly higher activity than the remaining ones. The composite materials **11–14** are more active catalysts for this reaction than the homogeneous counterparts **5–8**. Probably, the –Si(OEt)₃ groups present in the complexes, lead to the formation of less active or inactive oligomeric catalytic species [24].

Neither the pristine MCM host material **9** nor the DAB derivatized material **10** possess catalytic activity towards the ROMP

Table 3

Results for ROMP reaction of NBE and NBD initiated by isolated and immobilized [MX₂(CO)₃(L)₂] complexes

Catalyst	T (K)	PolyNBE		PolyNBD	
		Yield (%)	TOF ^a (g mol _M ⁻¹ h ⁻¹)	Yield (%)	TOF ^a (g mol _M ⁻¹ h ⁻¹)
[MoI ₂ (CO) ₃ (DAB)] (5)	328	5	11	2	4.7
[MoBr ₂ (CO) ₃ (DAB)] (6)	328	8	18	6	14
[WI ₂ (CO) ₃ (DAB)] (7)	328	2	5	1	2.3
[WBr ₂ (CO) ₃ (DAB)] (8)	328	3	7	2	4.7
MCM-DAB-MoI ₂ (11)	298	4	31	1	8.0
	328	15	117	6	48.0
MCM-DAB-MoBr ₂ (12)	298	12	94	6	48.0
	328	36	280	10	79.9
	328 ^b	24	211	–	–
	328 ^c	59	476	–	–
MCM-DAB-WI ₂ (13)	298	0.4	22	–	–
	328	1	55	–	–
MCM-DAB-WBr ₂ (14)	298	1.6	89	–	–
	328	3	166	–	–

^a Turnover frequency calculated at 72 h.

^b Second run.

^c In the presence of AlCl₃.

of the olefins, indicating that the active species must contain Mo or W. For all metal-containing catalysts, the ROMP of NBE is easier to accomplish than that of NBD. This is in agreement with literature results, where some authors reported that NBD is less readily polymerized than NBE [19]. The Mo-containing catalysts are more active than the tungsten analogues. The highest catalytic activity was observed for the derivatized material **12** (M=Mo, X=Br), giving TOF of $280 \text{ g mol}_{\text{Mo}}^{-1} \text{ h}^{-1}$ and $80 \text{ g mol}_{\text{Mo}}^{-1} \text{ h}^{-1}$ for ROMP of NBE and NBD, respectively. These results reflect the highest activity of complex **6** (M=Mo, X=Br) in homogeneous phase. In general, polymer yields obtained in the presence of the supported catalysts are better than those found for the corresponding unsupported complexes **5–8**, although the values are not very high (Table 3). They may be improved by increasing the reaction temperature. For example, in the case of **12**, a rise in temperature of 30 K leads to a three-fold increase in polyNBE yield.

It has been reported that the incorporation of aluminium in MCM, used as co-catalyst in metallocene systems, enhances the catalytic activity in ethene polymerization [33]. Accordingly, the performance of these catalysts may be improved by changing the support properties, by doping the silica-matrix with aluminium or by the addition of a co-catalyst, such as AlCl_3 . In order to check the effect of added aluminium, a catalytic reaction using material **12**, AlCl_3 , and NBE in the molar ratio of 1:3:200 at 328 K, was carried out. After 72 h, the reaction was stopped and the yield of polyNBE was estimated to be 59% with TOF of $476 \text{ g mol}_{\text{Mo}}^{-1} \text{ h}^{-1}$. This result is better than that obtained without AlCl_3 , indicating that the co-catalyst has a beneficial effect. It should, however, be mentioned that AlCl_3 alone did not show any catalytic activity.

The catalytic performance of catalyst **12** was also evaluated in a second reaction cycle. After reaction, the solid catalyst was separated from the reaction solution by filtration, and the polymer was precipitated by the addition of methanol. Both the conversion and polymer yield decreased from the first to the second run (Table 3). ICP-AES of the used and recovered solids showed that from the first to the second runs there is a 0.5% loss of metal, indicating that metal leaching does not occur to a great extent. The catalyst recovery procedure may be inefficient to remove all of the organic matter entrapped in the pore system, accounting for partial loss of catalytic activity observed upon recycling.

3. Conclusions

The immobilization of hepta-coordinate halocarbonyl Mo(II) and W(II) complexes on MCM was successfully accomplished by the tethering approach, using a phenyl-substituted 1,4-diazobutadiene spacer, and was confirmed by several techniques. For instance, the bands assigned to $\nu_{\text{C}\equiv\text{O}}$ modes observed by FTIR showed the incorporation of the organometallic $\text{M}(\text{CO})_3$ cores and the retention of their integrity. The immobilization of W(II) complexes inside the pores of the MCM-41 host material was not so successful as that of the Mo(II) analogues, according to the results of the metal loadings. While in homogeneous

phase complexes **5–8** exhibit poor catalytic activity (complex **6** (M=Mo, X=Br) being the most active), the catalytic performance of the corresponding heterogenized catalysts (**11–14**) in the ROMP of olefins is far superior. In general, the conversions are higher for NBE than for NBD. Nevertheless, the polymer yields achieved with the solid catalysts described in this work are, in general, relatively low. Polymer yield tends to increase with reaction temperature. The addition of AlCl_3 as a co-catalyst enhanced the catalytic performance of the material MCM-DAB-MoBr₂ (**12**) in the ROMP of NBE.

4. Experimental

4.1. General

All preparations and manipulations were performed using standard Schlenk techniques under nitrogen. Commercial grade solvents were dried and deoxygenated by standard procedures (Et_2O over Na/benzophenone ketyl; CH_2Cl_2 and CH_3CN over CaH_2), distilled under nitrogen and kept over 4 Å molecular sieves (3 Å for CH_3CN). Purely siliceous MCM was synthesized as described previously using $[(\text{C}_{16}\text{H}_{33})\text{N}(\text{CH}_3)_3]\text{Br}$ as the templating agent [24]. After calcinations (540 °C for 6 h), the material was characterized by powder XRD, N_2 adsorption and IR spectroscopy. Prior to the grafting experiment, physisorbed water was removed from calcined MCM by heating at 180 °C in vacuum (10^{-2} Pa) for 2 h. Microanalyses were performed at the University of Aveiro. BET specific surface areas (S_{BET} , p/p_0 from 0.03 to 0.13) and specific total pore volume, V_t , were estimated from N_2 adsorption isotherms measured at 77 K. The pore size distributions (PSD) were calculated by the BJH method using the modified Kelvin equation with correction for the statistical film thickness on the pore walls [34,35]. The statistical film thickness was calculated using Harkins–Jura equation in the p/p_0 range from 0.1 to 0.95.

Powder XRD data were collected on a Phillips PW1710 diffractometer using $\text{Cu K}\alpha$ radiation filtered by graphite. FTIR spectra in transmission mode were measured with a Mattson Satellite FTIR spectrometer using KBr pellets. ^1H and ^{13}C solution NMR spectra were obtained with a Bruker Avance-400 spectrometer. ^{29}Si and ^{13}C solid-state NMR spectra were recorded at 79.49 MHz and 100.62 MHz, respectively, on a (9.4 T) Bruker Avance 400P spectrometer. ^{29}Si MAS NMR spectra were recorded with 40° pulses, spinning rates 5.0–5.5 kHz, and 60 s recycle delays. ^{29}Si CP MAS NMR spectra were recorded with $5.5 \mu\text{s}$ 1H 90° pulses, 8 ms contact time, a spinning rate of 4.5 kHz, and 4 s recycle delays. ^{13}C CP MAS NMR spectra were recorded with a $4.5 \mu\text{s}$ 1H 90° pulse, 2 ms contact time, a spinning rate of 8 kHz, and 4 s recycle delays. Chemical shifts are quoted in ppm from TMS. ^{13}C spectra were also recorded in the solid-state at 125.76 MHz on a Bruker Avance 500 spectrometer. Phenyl-substituted 1,4-diazobutadiene ligand (DAB) was prepared as described previously [24]. The precursor organometallic complexes $\text{MoI}_2(\text{CO})_3(\text{NCCH}_3)_2$ (**1**), $\text{MoBr}_2(\text{CO})_3(\text{NCCH}_3)_2$ (**2**), $\text{WI}_2(\text{CO})_3(\text{NCCH}_3)_2$ (**3**) and $\text{WBr}_2(\text{CO})_3(\text{NCCH}_3)_2$ (**4**) were also prepared according to literature methods [25].

4.2. Catalytic studies

The complexes and materials reported herein were tested in the ROMP of NBE and NBD under N₂ atmosphere at 298 K and 328 K and using toluene as solvent. The polymers were precipitated by addition of methanol at the end of the reaction, i.e., after 72 h and upon catalyst separation. The catalytic reactions using complexes **5–8** were carried out using a catalyst/olefin molar ratio of 1:200. In the case of the studies using the composite materials **11–14** a metal/olefin molar ratio of 1:200 (based on the metal loadings as determined by ICP-AES) was used. For the catalytic reaction using AlCl₃ as co-catalyst the metal/Al/olefin molar ratio was 1:3:200. In a typical experiment, a certain amount of the materials with 18.5 mmol of olefin was mixed in toluene (10 ml) at 298 K or 328 K. All the reactions were stopped after 72 h. This was accomplished by separating the catalysts by filtration, followed by the addition of methanol to the toluene solution in order to precipitate the polymer. The solid polymer was separated by filtration and the polymers dried in vacuum before being weighed. The yields were calculated based on the initial weight of olefin used. The identification of the polymers was done by ¹H NMR [15–19].

4.3. Preparation of the complexes of type

[MX₂(CO)₃(DAB)] (M = Mo or W, and X = I or Br) (**5–8**)

A solution of **1–4** (0.50 mmol) in acetonitrile (10 ml) was treated with 1 equivalent of ligand DAB in acetonitrile (5 ml). The resulting turbid solution was stirred for 4 h at room temperature. The solvent was evaporated, and the solid product washed with hexane and dried in vacuum.

4.3.1. [MoI₂(CO)₃(DAB)] (**5**)

Yield: 85%. C₃₅H₅₂N₂Si₂O₉I₂Mo (1050.72) calcd: C 40.01, H 4.99, N 2.67; found: C 39.90, H 5.11, N 2.78. IR (KBr, ν cm⁻¹): 3058 (vw), 2973 (w), 2923 (vw), 2887 (vw), 2067 (vw), 2017 (m), 1946 (m), 1679 (m), 1637 (s), 1593 (s), 1492 (m), 1446 (s), 1400 (s), 1116 (vs), 1024 (vs), 952 (s), 764 (s), 698 (s). ¹H NMR (400.10 MHz, CDCl₃, r.t., δ ppm): 0.71 (s bd, 4H, SiCH₂), 1.04 (t, 18H, OCH₂CH₃), 1.93–1.98 (m, 4H, CH₂CH₂CH₂), 3.47–3.52 (m, 16H, NCH₂ and OCH₂CH₃), 7.36–7.95 (m, 10H, Ph). ¹³C NMR (100.25 MHz, CDCl₃, r.t., δ ppm): 13.1 (SiCH₂), 20.4 (OCH₂CH₃), 21.7 (CH₂CH₂CH₂), 58.1 (OCH₂CH₃), 68.7 (CH₂N=C), 127.2, 128.0, 128.9 (Ph) 166.7 (CH₂N=C).

4.3.2. [MoBr₂(CO)₃(DAB)] (**6**)

Yield: 72%. C₃₅H₅₂N₂Si₂O₉Br₂Mo (956.71) calcd: C 43.94, H 5.48, N 2.93; found: C 43.80, H 5.51, N 2.88. IR (KBr, ν cm⁻¹): 3057 (vw), 2978 (w), 2925 (vw), 2881 (vw), 2063 (w), 2011 (s), 1930 (vs), 1690 (m), 1635 (s), 1594 (s), 1444 (s), 1396 (s), 1167 (m), 1075 (vs), 957 (vs), 766 (s), 707 (m). ¹H NMR (400.10 MHz, CDCl₃, r.t., δ ppm): 0.71–0.86 (m, 4H, SiCH₂), 1.05 (t, 18H, OCH₂CH₃), 1.93–1.98 (m, 4H, CH₂CH₂CH₂), 3.48–3.53 (m, 16H, NCH₂ and OCH₂CH₃), 7.31–7.97 (m, 10H, Ph). ¹³C NMR (100.25 MHz, CDCl₃, r.t., δ ppm): 10.5 (SiCH₂), 18.8 (OCH₂CH₃), 23.3 (CH₂CH₂CH₂), 57.5 (OCH₂CH₃), 66.4 (CH₂N=C), 126.9, 128.3, 129.1 (Ph), 166.3 (CH₂N=C).

4.3.3. [WI₂(CO)₃(DAB)] (**7**)

Yield: 48%. C₃₅H₅₂N₂Si₂O₉I₂W (1138.62) calcd: C 36.92, H 4.60, N 2.46; found: C 37.06, H 4.71, N 2.58. IR (KBr, ν cm⁻¹): 3056 (vw), 2976 (w), 2935 (w), 2025 (vw), 1980 (s), 1934 (s), 1633 (s), 1451 (w), 1246 (vs), 1081 (vs), 950 (s), 796 (m), 693 (w). ¹H NMR (400.10 MHz, CDCl₃, r.t., δ ppm): 0.66 (s bd, 4H, SiCH₂), 1.15–1.31 (m, 18H, OCH₂CH₃), 1.72–1.90 (m, 4H, CH₂CH₂CH₂), 3.32–3.34 (m, 4H, NCH₂), 3.69–3.81 (m, 12H, OCH₂CH₃), 7.31–7.75 (m, 5H, Ph), 7.57–7.75 (m, 3H, Ph), 7.88–7.93 (m, 2H, Ph). ¹³C NMR (100.25 MHz, CDCl₃, r.t., δ ppm): 9.2 (SiCH₂), 19.8 (OCH₂CH₃), 24.8 (CH₂CH₂CH₂), 55.9 (CH₂N=C), 57.8 (OCH₂CH₃), 127.6, 128.9, 129.4 (Ph), 165.6 (CH₂N=C).

4.3.4. [WBr₂(CO)₃(DAB)] (**8**)

Yield: 58%. C₃₅H₅₂N₂Si₂O₉Br₂W (1044.61) calcd: C 40.24, H 5.02, N 2.68; found: C 40.11, H 5.11, N 2.79. IR (KBr, ν cm⁻¹): 3067 (vw), 2986 (w), 2930 (vw), 2032 (vw), 1985 (s), 1940 (m), 1649 (s), 1234 (vs), 1076 (vs), 978 (vs), 791 (m), 700 (w). ¹H NMR (400.10 MHz, CDCl₃, r.t., δ ppm): 0.74–0.85 (s bd, 4H, SiCH₂), 1.19 (t, 18H, OCH₂CH₃), 1.78–1.85 (m, 4H, CH₂CH₂CH₂), 3.20–3.30 (t, 4H, NCH₂), 3.61–3.73 (m, 12H, OCH₂CH₃), 7.48 (s bd, 2H, Ph), 7.58–7.62 (m, 5H, Ph), 7.73–7.87 (m, 3H, Ph). ¹³C NMR (100.25 MHz, CDCl₃, r.t., δ ppm): 8.7 (SiCH₂), 19.1 (OCH₂CH₃), 23.6 (CH₂CH₂CH₂), 57.3 (CH₂N=C), 58.4 (OCH₂CH₃), 126.9, 128.9, 129.6 (Ph), 166.5 (CH₂N=C).

4.4. MCM-DAB (**10**)

A solution of ligand DAB (0.70 g, 1.13 mmol) in toluene (10 ml) was added to a suspension of MCM-41 (0.8 g) in toluene (10 ml) and the mixture heated at 100 °C for 9 h. The resultant solid was then filtered off and washed four times with CH₂Cl₂ (4 × 15 ml), and dried in vacuum at 50 °C for 3 h. Elemental analysis found (%): C 16.20, N 1.50, H 2.80. IR (KBr, ν cm⁻¹): 3067 (vw), 2978 (w), 2927 (vw), 2891 (vw), 1652 (s), 1494 (s), 1447 (s), 1390 (m), 1245 (vs), 1080 (vs), 951 (s), 800 (s), 702 (m). ¹³C CP/MAS NMR (δ ppm): 8.8 (SiCH₂), 16.2, 20.5, 41.6, 57.5, 128.1 (Ph-C). ²⁹Si MAS NMR (δ ppm): -55.4 (T¹), -109.5 (Q⁴). ²⁹Si CP/MAS NMR (δ ppm): -54.9 (T¹), -59.6 (T²), -67.0 (T³), -91.9 (Q²), -101.9 (Q³), -109.2 (Q⁴).

4.5. Preparation of the materials of the type MCM-DAB-MX₂ (**11–14**)

A solution of **1–4** (0.4 mmol) in CH₂Cl₂ (10 ml) was added to a suspension of **10** (1.0 g) in CH₂Cl₂ (10 ml) and the mixture stirred at room temperature for 24 h. The solution was filtered off and the pale yellow powder washed repeatedly with CH₂Cl₂ (4 × 20 ml), before drying under vacuum at room temperature for several hours.

4.5.1. MCM-DAB-MoI₂ (**11**)

Elemental analysis found (%): C 13.60, N 1.45, H 2.74, Mo 2.6. IR (KBr, ν cm⁻¹): 3072 (vw), 2978 (w), 2932 (vw), 2896 (vw), 2073 (vw), 2022 (m), 1954 (m), 1631 (s), 1494

(s), 1447 (s), 1400 (m), 1241 (vs), 1080 (vs), 945 (m), 806 (s), 702 (m). ^{13}C CP/MAS NMR (δ ppm): 10.0 (SiCH₂), 16.8, 21.2, 42.9, 58.0, 129.5 (Ph-C). ^{29}Si MAS NMR (δ ppm): -55.8 (T^1), -110.0 (Q^4). ^{29}Si CP/MAS NMR (δ ppm): -53.9 (T^1), -60.0 (T^2), -67.7 (T^3), -92.8 (Q^2), -102.6 (Q^3), -109.7 (Q^4).

4.5.2. MCM-DAB-MoBr₂ (I2)

Elemental analysis found (%): C 13.60, N 1.45, H 2.68, Mo 2.8. IR (KBr, ν cm⁻¹): 3062 (vw), 2977 (w), 2082 (vw), 2018 (m), 1944 (m), 1627 (s), 1499 (m), 1451 (m), 1403 (m), 1234 (vs), 1034 (vs), 943 (s), 800 (m), 705 (w). ^{13}C CP/MAS NMR (δ ppm): 9.5 (SiCH₂), 16.7, 21.0, 42.7, 57.9, 129.1 (Ph-C). ^{29}Si MAS NMR (δ ppm): -53.8 (T^1), -109.7 (Q^4). ^{29}Si CP/MAS NMR (δ ppm): -55.5 (T^1), -60.1 (T^2), -68.8 (T^3), -92.8 (Q^2), -102.2 (Q^3), -109.7 (Q^4).

4.5.3. MCM-DAB-WI₂ (I3)

Elemental analysis found (%): C 15.88, N 1.53, H 2.91, W 0.4. IR (KBr, ν cm⁻¹): 3062 (vw), 2977 (w), 2924 (vw), 2029 (vw), 1987 (w), 1959 (m), 1632 (s), 1447 (w), 1399 (w), 1235 (s), 1076 (vs), 948 (m), 800 (m), 700 (w). ^{13}C CP/MAS NMR (δ ppm): 9.6 (SiCH₂), 16.8, 20.9, 42.3, 57.5, 129.4 (Ph-C). ^{29}Si MAS NMR (δ ppm): -53.4 (T^1), -109.6 (Q^4). ^{29}Si CP/MAS NMR (δ ppm): -53.9 (T^1), -59.9 (T^2), -64.5 (T^3), -92.0 (Q^2), -101.9 (Q^3), -109.6 (Q^4).

4.5.4. MCM-DAB-WBr₂ (I4)

Elemental analysis found (%): C 18.23, N 1.53, H 3.22, W 0.7. IR (KBr, ν cm⁻¹): 3067 (vw), 2980 (w), 2929 (vw), 2891 (vw), 2058 (vw), 2020 (w), 1958 (m), 1632 (s), 1450 (m), 1388 (w), 1244 (m), 1075 (vs), 800 (s), 700 (m). ^{13}C CP/MAS NMR (δ ppm): 9.8 (SiCH₂), 17.1, 20.8, 42.5, 57.7, 128.6 (Ph-C). ^{29}Si MAS NMR (δ ppm): -55.2 (T^1), -109.6 (Q^4). ^{29}Si CP/MAS NMR (δ ppm): -54.7 (T^1), -60.4 (T^2), -67.5 (T^3), -91.6 (Q^2), -102.0 (Q^3), -109.7 (Q^4).

Acknowledgments

CDN (SFRH/BPD/14512/2003) and PDV (SFRH/BPD/14903/2004) thank FCT for research grants. JG thanks the Socrates Student Exchange Program for a grant. Paula Brandão is acknowledged for assistance with the NMR experiments.

Appendix A. Supplementary data

Supplementary data associated with this article can be found, in the online version, at doi:10.1016/j.molcata.2006.04.023.

References

- [1] M.H. Valkenberg, W.F. Hölderich, Catal. Rev. 44 (2002) 321.
- [2] A. Taguchi, F. Schüth, Micropor. Mesopor. Mater. 77 (2005) 1.
- [3] P.K. Baker, Chem. Soc. Rev. 27 (1998) 129.
- [4] H. Liu, M.J. Calhorda, V. Félix, M.G.B. Drew, J. Organomet. Chem. 632 (2001) 175.
- [5] H. Liu, M.J. Calhorda, V. Félix, M.G.B. Drew, L.F. Veiros, Inorg. Chim. Acta 327 (2002) 169.
- [6] R. Colton, I.B. Tomkins, Aust. J. Chem. 19 (1966) 1143.
- [7] D.P. Tate, W.R. Knipple, J.M. Augl, Inorg. Chem. 1 (1962) 433.
- [8] A.D. Westland, N. Muriithi, Inorg. Chem. 11 (1972) 2971.
- [9] P.K. Baker, Adv. Organomet. Chem. 40 (1996) 45.
- [10] M.G.B. Drew, Prog. Inorg. Chem. 23 (1977) 67.
- [11] M. Melník, P. Sharrock, Coord. Chem. Rev. 65 (1985) 49.
- [12] H.L. Nigam, R.S. Nyholm, Proc. Chem. Soc. (1957) 321.
- [13] L. Bencze, A. Kraut-Vass, J. Mol. Catal. 28 (1985) 369.
- [14] L. Bencze, A. Kraut-Vass, L. Prókai, J. Chem. Soc. Chem. Commun. (1985) 911.
- [15] M. Al-Jahdali, P.K. Baker, A.J. Lavery, M. Meehan, D.J. Muldoon, J. Mol. Catal. A: Chem. 159 (2000) 51.
- [16] P.K. Baker, M.A. Beckett, B.M. Stiefvater-Thomas, J. Mol. Catal. A: Chem. 193 (2003) 77.
- [17] T. Szymańska-Buzar, T. Glowiak, I. Czeluśniak, J. Organomet. Chem. 640 (2001) 72.
- [18] T. Szymańska-Buzar, T. Glowiak, I. Czeluśniak, Polyhedron 21 (2002) 2505.
- [19] I. Czeluśniak, T. Szymańska-Buzar, Appl. Catal. A 277 (2004) 173.
- [20] C.T. Kresge, M.E. Leonowicz, W.J. Roth, J.C. Vartuli, J.S. Beck, Nature 359 (1992) 710.
- [21] J.S. Beck, J.C. Vartuli, W.J. Roth, M.E. Leonowicz, C.T. Kresge, K.D. Schmitt, C.T.-W. Chu, D.H. Olson, E.W. Sheppard, S.B. McCullen, J.B. Higgins, J.L. Schlenker, J. Am. Chem. Soc. 114 (1992) 10834.
- [22] B. Hatton, K. Landskron, W. Whitnall, D. Perovic, G.A. Ozin, Acc. Chem. Res. 38 (2005) 305.
- [23] A. Corma, Chem. Rev. 97 (1997) 2373.
- [24] C.D. Nunes, M. Pillinger, A.A. Valente, J. Rocha, A.D. Lopes, I.S. Gonçalves, Eur. J. Inorg. Chem. (2003) 3870.
- [25] P.K. Baker, S.G. Fraser, E.M. Keys, J. Organomet. Chem. 309 (1986) 319.
- [26] C.D. Nunes, M. Pillinger, A.A. Valente, A.D. Lopes, I.S. Gonçalves, Inorg. Chem. Commun. 6 (2003) 1228.
- [27] B. Marler, U. Oberhagemann, S. Voltmann, H. Gies, Micropor. Mater. 6 (1996) 375.
- [28] W. Hammond, E. Prouzet, S.D. Mahanti, T.J. Pinnavaia, Micropor. Mesopor. Mater. 27 (1999) 19.
- [29] S.J. Gregg, K.S.W. Sing, Adsorption, Surface Area and Porosity, second ed., Academic Press, London, 1982.
- [30] M.D. Alba, A. Becerro, J. Klinowski, J. Chem. Soc., Faraday Trans. 92 (1996) 849.
- [31] A.A. Romero, M.D. Alba, W. Zhou, J. Klinowski, J. Phys. Chem. B 101 (1997) 5294.
- [32] M. Kruk, M. Jaroniec, Langmuir 15 (1999) 5410.
- [33] H. Rahiala, I. Beurroies, T. Eklund, K. Hakala, R. Gougeon, P. Trems, J.B. Rosenholm, J. Catal. 188 (1999) 14.
- [34] M. Kruk, M. Jaroniec, Langmuir 13 (1997) 6267.
- [35] M. Kruk, V. Antochshuk, M. Jaroniec, J. Phys. Chem. B 103 (1999) 10670.